

# Universally optimal verification of entangled states with non-demolition measurements

Ye-Chao Liu,<sup>1</sup> Jiangwei Shang,<sup>1,\*</sup> Rui Han,<sup>2</sup> and Xiangdong Zhang<sup>1,†</sup>

<sup>1</sup>*Key Laboratory of Advanced Optoelectronic Quantum Architecture and Measurement of Ministry of Education, School of Physics, Beijing Institute of Technology, Beijing 100081, China*

<sup>2</sup>*Centre for Quantum Technologies, National University of Singapore, Singapore 117543, Singapore*

(Dated: September 21, 2022)

The efficient and reliable characterization of quantum states plays a vital role in most, if not all, quantum information processing tasks. In this work, we present a universally optimal protocol for verifying entangled states by employing the so-called quantum non-demolition measurements, such that the verification efficiency is equivalent to that of the optimal global strategy. Instead of being probabilistic as the standard verification strategies, our protocol is constructed sequentially, which is thus more favorable for experimental realizations. In addition, the target states are preserved in the protocol after each measurement, so can be reused in any subsequent tasks. We demonstrate the power of our protocol for the optimal verification of Bell states, arbitrary two-qubit pure states, and stabilizer states. We also prove that our protocol is able to perform tasks including fidelity estimation and state preparation.

*Introduction.*—One basic yet important step in almost all quantum information processing tasks is to efficiently and reliably characterize the quantum states. However, the standard tool of quantum state tomography [1] is typically rather time-consuming and computationally hard due to the exponentially increasing number of parameters to be reconstructed [2, 3]. Thus, much attention has been drawn to the quest for nontomographic methods [4–8], among which quantum state verification (QSV) [9] particularly stands out because of its many notable properties including its high efficiency and low cost of resources. Up to now, it has been shown that a large variety of bipartite and multipartite quantum states [9–24] can be verified efficiently or even optimally by QSV. Very recently, efficient protocols for verifying quantum processes (including quantum gates and quantum measurements) have also been proposed [25–27].

In short, QSV is a procedure for gaining confidence that the output of a quantum device is a particular target state  $|\psi\rangle$  over any others using local measurements. A QSV protocol  $\Omega$  takes on the general form

$$\Omega = \sum_i \mu_i \Omega_i, \quad (1)$$

where  $\{\Omega_i, \mathbb{1} - \Omega_i\}$  is a set of two-outcome tests carried out with probability  $\{\mu_i\}$ . The projective operators  $\Omega_i$ s satisfy  $\Omega_i|\psi\rangle = |\psi\rangle$  for all  $i$ . If all  $N$  states passed the test, we achieve the confidence level  $1 - \delta$  with  $\delta \leq [1 - \epsilon\nu(\Omega)]^N$ , where  $\epsilon$  is the infidelity of the states and  $\nu(\Omega) := 1 - \lambda_2(\Omega)$  denotes the spectral gap between the largest and the second largest eigenvalues of  $\Omega$  [9, 21]. Hence, the QSV protocol  $\Omega$  can verify  $|\psi\rangle$  to infidelity  $\epsilon$  and confidence level  $1 - \delta$  with the number of copies of the states satisfying

$$N \geq \frac{\ln \delta^{-1}}{\ln \{[1 - \nu(\Omega)\epsilon]^{-1}\}} \approx \frac{1}{\nu(\Omega)} \epsilon^{-1} \ln \delta^{-1}. \quad (2)$$

Compared with tomography as well as other nonto-

mographic methods, properly engineered QSV protocols can greatly reduce the cost of resources. Additionally,  $\Omega_i$ s are expected to be implementable with local measurements only, thus facilitating the ease of experimental realizations. However, there remains three major issues associated with QSV. The first one concerns its efficiency, where an optimal strategy can rarely (if not impossible at all) be devised. Secondly, the measurements  $\{\Omega_i\}$  are implemented in a probabilistic manner with probability distribution  $\{\mu_i\}$ , which can be very difficult to handle in experiments [19, 23]. Lastly, the unknown quantum states to be characterized are destroyed after each measurement as the system collapses at the detector, thus, cannot be reused in any subsequent tasks. In fact, the latter two issues with QSV also exist in tomography and many other nontomographic methods.

In this work, we propose a new type of protocol to tackle *all* these issues associated with QSV. Our protocol is based on the so-called quantum non-demolition (QND) measurement [28–30], which is the type of measurement that leaves the post-measurement quantum states undestroyed, thus allowing repeated or sequential measurements. We fully explore the use of sequentially constructed QND measurements for state verification instead of the probabilistic construction as in the standard QSV strategies. Under such a scheme, not only can we preserve the target states, but also manage to universally reach the efficiency of the optimal global strategy. Specifically, in order to verify the target state within infidelity  $\epsilon$  and confidence level  $1 - \delta$ , we only need  $N \approx \epsilon^{-1} \ln \delta^{-1}$  copies of the states. In addition, our protocol is robust in the sense that the sequence of measurements can be constructed in an arbitrary order which is rather friendly to experimental implementations. We demonstrate the power of our protocol for the optimal verification of Bell states, arbitrary two-qubit pure states, and stabilizer states. Last but not least, we prove that the protocol can also be used to perform other tasks including fidelity

estimation and state preparation.

*Non-demolition quantum verification.*—The QND measurements are often realized through the entanglement with an ancilla system followed by a measurement on the ancilla. Let us consider the joint system-ancilla state  $|\psi\rangle\otimes|0\rangle$ , where the ancilla qubit is initially prepared in state  $|0\rangle$ . Next, we entangle the system and the ancilla via the following operation

$$U_i = \Omega_i \otimes \mathbb{1} + (\mathbb{1} - \Omega_i) \otimes X, \quad (3)$$

and obtain

$$|\psi_i\rangle := \Omega_i|\psi\rangle \otimes |0\rangle + (\mathbb{1} - \Omega_i)|\psi\rangle \otimes |1\rangle, \quad (4)$$

where  $\{\Omega_i, \mathbb{1} - \Omega_i\}$  are the “pass-or-fail” tests for verifying  $|\psi\rangle$  in the standard QSV. Note that the unitarity of  $U_i$  is ensured since  $\Omega_i$  is a projector. With this operation, performing a Pauli- $Z$  measurement on the ancilla qubit of the coupled state  $|\psi_i\rangle$  is effectively equivalent to the realization of the two-outcome measurement  $\{\Omega_i, \mathbb{1} - \Omega_i\}$  on the system. This procedure can be concisely described by the operation

$$\mathcal{M}_i = (\mathbb{1} \otimes |0\rangle\langle 0|) U_i \quad (5)$$

on the joint system  $|\psi\rangle\otimes|0\rangle$ , which is a QND measurement on the system state  $|\psi\rangle$ . Note that  $\mathcal{M}_i$  corresponds to a positive operator-valued measure, and is usually not hermitian.

It can be easily checked  $\mathcal{M}_i(|\psi\rangle\otimes|0\rangle) = |\psi\rangle\otimes|0\rangle$  for all  $i$ . Therefore, verifying the target state  $|\psi\rangle$  by  $\Omega_i$  is exactly the same as verifying  $|\psi\rangle$  non-destructively using  $\mathcal{M}_i$ . In this way, we reformulate the procedure of QSV using QND measurements with the addition of ancilla qubits, which we dub as *non-demolition quantum verification* (NDQV). Here we have two quick remarks. First, due to the dichotomic nature of the measurements  $\{\Omega_i, \mathbb{1} - \Omega_i\}$  on the system, the coupled ancilla can always be chosen as a two-dimensional qubit, no matter what the dimension of the target system is [31]. Second, the entangling operation  $U_i$  is of a similar structure to those used in many other applications such as quantum error correction [32–36] and can be realized with standard quantum gates.

*Sequential NDQV.*—The NDQV protocol can, of course, be implemented in a probabilistic manner as that of the standard QSV. However, doing so would be a waste of resources as the key advantage of the NDQV protocol lies in the fact that the target state is not destroyed and remains undisturbed as long as the test passes. Thus, the post-measurement state can be reliably used and measured again. Forasmuch, we introduce the so-called *sequential* NDQV protocol; see below the theorem.

**Theorem 1.** *If a target state  $|\psi\rangle$  can be verified by the protocol  $\Omega = \sum_i \mu_i \Omega_i$ , where  $\Omega_i$ s are local projectors,*

*then it can be verified optimally by*

$$\mathcal{M} = \prod_i \mathcal{M}_i \quad (6)$$

*with  $\mathcal{M}_i$  being defined by Eqs. (5) and (3). The spectral gap of  $\mathcal{M}$  is given by*

$$\nu(\mathcal{M}) = 1, \quad (7)$$

*indicating that the verification efficiency of  $\mathcal{M}$  is the same as that of the optimal global strategy.*

*Proof.* Same as the standard QSV protocol, the spectral gap is given by  $\nu(\mathcal{M}) := 1 - \lambda_2(\mathcal{M})$  with  $\lambda_2(\mathcal{M})$  being the second largest eigenvalue of  $\mathcal{M}$ ; see the explicit derivation in Appendix A. With  $\mathcal{M}_i$  being defined as in Eqs. (5) and (3), we have

$$\begin{aligned} \mathcal{M} &= \prod_i [\Omega_i \otimes |0\rangle\langle 0| + (\mathbb{1} - \Omega_i) \otimes |0\rangle\langle 1|] \\ &= \prod_i \Omega_i \otimes |0\rangle\langle 0| + \prod_{i \neq l} \Omega_i \cdot (\mathbb{1} - \Omega_l) \otimes |0\rangle\langle 1|, \end{aligned} \quad (8)$$

where the  $l$ th setting is first chosen to be performed in the sequence. Here the operators  $|0\rangle\langle 0|$  and  $|0\rangle\langle 1|$  act on the entire pool of ancilla qubits for all the measurement settings. The second term in Eq. (8) does not affect the eigendecomposition of  $\mathcal{M}$ , thus one has  $\nu(\mathcal{M}) = \nu(\prod_i \Omega_i)$ . To be able to verify the target state  $|\psi\rangle$ , each projector  $\Omega_i$  should take on the general form

$$\Omega_i = |\psi\rangle\langle\psi| + \sum_p \lambda_i^p |\psi^p\rangle\langle\psi^p|, \quad (9)$$

where the basis  $\{|\psi^p\rangle\}$  spans the subspace orthogonal to  $|\psi\rangle$ . Since  $\Omega_i$  is constructed by local projectors, we must have  $\lambda_i^p = 0$  or  $1$ ,  $\forall(i, p)$ . Therefore, for a complete verification protocol, we have

$$\Omega_s := \prod_i \Omega_i = |\psi\rangle\langle\psi|, \quad (10)$$

and  $\nu(\mathcal{M}) = \nu(\Omega_s) = 1$ .  $\square$

Several remarks about the sequential NDQV protocol are in order. Firstly, since the initial ancilla qubit state is fixed to be  $|0\rangle$ , following Eq. (8) one has

$$\mathcal{M}(\sigma \otimes |0\rangle\langle 0|) = (\Omega_s \otimes \mathbb{1})(\sigma \otimes |0\rangle\langle 0|) \quad (11)$$

for verifying an arbitrary state  $\sigma$ . Thus, we can write the sequential NDQV measurement as

$$\mathcal{M} \hat{=} \Omega_s \otimes \mathbb{1}, \quad (12)$$

where the symbol “ $\hat{=}$ ” denotes the conditional equivalence when the ancilla qubits are initially prepared in state  $|0\rangle$ , which is always the case for our NDQV protocol. In addition, the order of the measurements  $\mathcal{M}_i$ s

in the sequential NDQV protocol can be made arbitrary. This can be easily deduced from Eq. (8) because the order of the measurements only affects the second term which is irrelevant to the eigendecomposition of  $\mathcal{M}$ . This makes the sequential NDQV protocol potentially rather friendly to experimental implementations.

Secondly, the optimality of the sequential NDQV protocol directly leads us to the following corollary regarding efficiency.

**Corollary 1.** *The verification efficiency of the sequential NDQV protocol will not be improved by adding more measurement settings.*

Rather than taking it as the direct consequence of the optimality property, we prove this corollary by direct calculations in Appendix B. This property of the sequential NDQV protocol is very different from that of the standard QSV strategies where more measurement settings usually can improve the verification efficiency [9]. In other words, our protocol provides a universal upper bound for the minimal number of measurement settings demanded for state verification.

Lastly, the sequential NDQV protocol offers us two additional by-products, namely, fidelity estimation and state preparation; see below the corollary.

**Corollary 2.** *The average fidelity between the output state  $\sigma$  and the target state  $|\psi\rangle$ , i.e.,  $\mathcal{F} = \langle F \rangle$ , can be directly estimated by the sequential NDQV protocol,*

$$\mathcal{M}(\sigma \otimes |0\rangle\langle 0|) = F|\psi\rangle\langle\psi| \otimes |0\rangle\langle 0|, \quad (13)$$

where  $F = \langle\psi|\sigma|\psi\rangle$  is the fidelity between  $\sigma$  and  $|\psi\rangle$ .

In addition, Eq. (13) also implies that, with a certain probability  $\mathcal{F}$ , the target state  $|\psi\rangle$  is preserved after the measurements. Hence, the sequential NDQV protocol can be regarded as a state preparation process, with the successful rate given by the average fidelity between the output state and the target state.

*Bell state verification.*—Consider the case of verifying the Bell state  $|\Phi\rangle = (|00\rangle + |11\rangle)/\sqrt{2}$ . In the standard QSV protocol  $\Omega_{\text{Bell}}$ , this state can be verified efficiently using two measurement settings [9] with

$$\begin{aligned} \Omega_1 &= P_{ZZ}^+ = |0\rangle\langle 0| \otimes |0\rangle\langle 0| + |1\rangle\langle 1| \otimes |1\rangle\langle 1|, \\ \Omega_2 &= P_{XX}^+ = |+\rangle\langle +| \otimes |+\rangle\langle +| + |- \rangle\langle -| \otimes |- \rangle\langle -|, \end{aligned} \quad (14)$$

where  $|\pm\rangle = (|0\rangle \pm |1\rangle)/\sqrt{2}$ . Taking  $\Omega_{\text{Bell}} = \frac{1}{2}(\Omega_1 + \Omega_2)$ , the corresponding spectral gap is given by  $\nu(\Omega_{\text{Bell}}) = \frac{1}{2}$ .

Using Theorem 1, we construct the sequential NDQV protocol for verifying  $|\Phi\rangle$  as  $\mathcal{M}_{\text{Bell}} = \mathcal{M}_1 \mathcal{M}_2$  (or equivalently as  $\mathcal{M}_{\text{Bell}} = \mathcal{M}_2 \mathcal{M}_1$ ). The two QND measurement settings  $\mathcal{M}_{1(2)}$  are defined as in Eq. (5) with

$$\begin{aligned} U_1 &= P_{ZZ}^+ \otimes \mathbb{1} + (\mathbb{1} - P_{ZZ}^+) \otimes X \\ &= \mathcal{C}_{X1a} \mathcal{C}_{X2a}, \\ U_2 &= P_{XX}^+ \otimes \mathbb{1} + (\mathbb{1} - P_{XX}^+) \otimes X \\ &= (H \otimes H \otimes \mathbb{1}) \mathcal{C}_{X1a} \mathcal{C}_{X2a} (H \otimes H \otimes \mathbb{1}), \end{aligned} \quad (15)$$

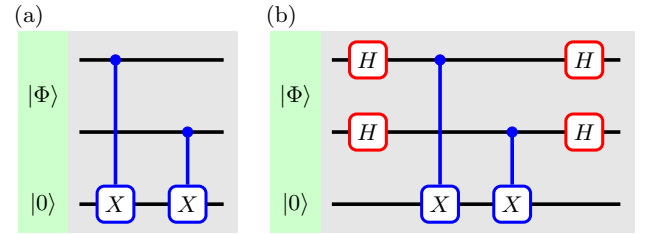


FIG. 1. Circuits for the experimental realization of the coupling operations  $U_1$  (a) and  $U_2$  (b) as in Eq. (15).  $|\Phi\rangle$  is the target Bell state to be verified, and  $|0\rangle$  represents the ancilla qubit.

where  $H$  is the Hadamard gate, and  $\mathcal{C}_{Xja}$  denotes the CNOT gate that the ancilla qubit  $a$  is controlled by the  $j$ th qubit. The corresponding circuits for the experimental realization of the coupling operations  $U_{1(2)}$  are illustrated in Fig. 1.

Specifically, the sequential NDQV protocol for verifying the Bell state  $|\Phi\rangle$  proceeds as follows. Together with an ancilla qubit prepared in state  $|0\rangle$ , the actual state  $\sigma$  is sent into the circuit for the coupling operation  $U_1$ , followed by a Pauli-Z measurement on the ancilla at the end of the circuit. If the measurement outcome is  $|0\rangle$ , together with another freshly prepared ancilla qubit in state  $|0\rangle$ , the system state is passed on to the circuit for the coupling operation  $U_2$  followed by a Pauli-Z measurement on the ancilla. If the outcome is still  $|0\rangle$ , we declare the test passes. In any other cases, we say that the test fails. In this way, the protocol  $\mathcal{M}_{\text{Bell}}$  has a spectral gap  $\nu(\mathcal{M}_{\text{Bell}}) = 1$ , which is equivalent to the optimal global strategy, and  $N \approx \epsilon^{-1} \ln \delta^{-1}$  number of copies of the state are required to verify  $|\Phi\rangle$  within infidelity  $\epsilon$  and confidence level  $1 - \delta$ .

One final remark concerning the verification efficiency is that, in the standard QSV protocol, the efficiency can be further improved to  $\nu(\Omega'_{\text{Bell}}) = \frac{2}{3}$  by adding an additional measurement setting  $P_{YY}^-$  [9, 18]. However, by Corollary 1, more measurement settings will not help improve the sequential NDQV protocol as it is already equivalent to the optimal global strategy.

*Verification of arbitrary two-qubit pure states.*—Without loss of generality, we write the two-qubit entangled pure state as  $|\Psi\rangle = \sin \theta |00\rangle + \cos \theta |11\rangle$  with  $\theta \in (0, \pi/4)$ . In the standard QSV protocol, this state can be verified efficiently using three local settings [18],

$$\begin{aligned} \Omega_1 &= P_{ZZ}^+ = |0\rangle\langle 0| \otimes |0\rangle\langle 0| + |1\rangle\langle 1| \otimes |1\rangle\langle 1|, \\ \Omega_2 &= \mathbb{1} - |+\rangle\langle +| \otimes |\varphi_+\rangle\langle\varphi_+|, \\ \Omega_3 &= \mathbb{1} - |- \rangle\langle -| \otimes |\varphi_-\rangle\langle\varphi_-|, \end{aligned} \quad (16)$$

where  $|\varphi_\pm\rangle = \cos \theta |0\rangle \mp \sin \theta |1\rangle$ . The corresponding spectral gap is  $\nu(\Omega_{2\text{qb}}) = \frac{1}{3}$  by taking  $\Omega_{2\text{qb}} = \frac{1}{3} \sum_{i=1}^3 \Omega_i$ . The efficiency can be improved by other QSV protocols with

different measurement settings. More details on the standard QSV protocols can be found in Appendix C, where we also discuss how to do the verification using adaptive methods. Then in Appendix D, we show how to realize the corresponding adaptive QND measurements.

By applying Eqs. (5) and (3), we find that the QND implementation of Eq. (16) is given by

$$\begin{aligned}\mathcal{M}_1 &= (\mathbb{1} \otimes |0\rangle\langle 0|) \mathcal{C}_{X1a} \mathcal{C}_{X2a}, \\ \mathcal{M}_i^t &= (\mathbb{1} \otimes |0\rangle\langle 0|) (R_i^\dagger \otimes \mathbb{1}) (X \otimes X \otimes \mathbb{1}) \\ &\quad \mathcal{C}_{X12a}^2 (X \otimes X \otimes \mathbb{1}) (R_i \otimes \mathbb{1}),\end{aligned}\quad (17)$$

for  $i = \{2, 3\}$ , where the rotation matrix  $R_{2(3)}$  turns the state  $|+\rangle \otimes |\varphi_+\rangle$  ( $|-\rangle \otimes |\varphi_-\rangle$ ) into  $|00\rangle$ . Specifically,

$$R_2 = H \otimes \begin{bmatrix} \cos \theta & -\sin \theta \\ \sin \theta & \cos \theta \end{bmatrix} \text{ and } R_3 = XH \otimes \begin{bmatrix} \cos \theta & \sin \theta \\ -\sin \theta & \cos \theta \end{bmatrix}. \quad (18)$$

These QND measurements require a Toffoli (CCNOT) gate  $\mathcal{C}_{X12a}^2$  which is a three-body coupling operation. For systems where the Toffoli gate is not easily accessible, in this setting of NDQV, one can also effectively replace it with two CNOT gates using two ancilla qubits initially prepared in  $|00\rangle$ . We denote the new set of QND measurements by  $\mathcal{M}_i^b$  and, for  $i = \{2, 3\}$ ,

$$\mathcal{M}_i^b = \mathbb{1} - (\mathbb{1} \otimes |00\rangle\langle 00|) (R_i^\dagger \otimes \mathbb{1}) \mathcal{C}_{X1a} \mathcal{C}_{X2a'} (R_i \otimes \mathbb{1}). \quad (19)$$

The equivalence of the two NDQV protocols  $\mathcal{M}^t = \mathcal{M}_1 \mathcal{M}_2^t \mathcal{M}_3^t$  and  $\mathcal{M}^b = \mathcal{M}_1 \mathcal{M}_2^b \mathcal{M}_3^b$  (or arbitrary permutations of each of the three measurement settings) can be obtained from  $\mathcal{M}_i^t \cong \mathcal{M}_i^b$  by direct calculations, and both of them are equivalent to the optimal global strategy. The latter replaces the Toffoli gate by two CNOT gates at the cost of one additional ancilla qubit. In fact, this equivalence also holds for many-body coupling operations; see below the proposition with the proof shown in Appendix E.

**Proposition 2.** *For the specific setting of NDQV where the ancilla is always prepared in  $|0\rangle$  and measured in the Pauli-Z basis, a generalized  $(n+1)$ -body Toffoli gate can always be replaced by  $n$  two-body CNOT gates with ancilla qubits initially prepared in  $|0\rangle^{\otimes n}$ .*

*Verification of stabilizer states.*—Stabilizer states, such as the GHZ states [32, 37], are an important class of multipartite states. An  $n$ -qubit stabilizer state  $|\psi\rangle$  can be determined by a stabilizer group  $\mathcal{S}$ , where  $\mathcal{S}$  is generated by a set of  $n$  commuting Pauli operators  $\{S_1, \dots, S_n\}$  (the stabilizer generators). With  $S_i|\psi\rangle = |\psi\rangle$  for all  $i$ , the stabilizer group uniquely defines the state  $|\psi\rangle$ .

In the standard QSV strategy, an  $n$ -qubit stabilizer state can be verified with efficiency  $\nu = 1/n$  using minimally  $n$  measurement settings that are constructed according to the stabilizer generators of the corresponding state [9]. This verification efficiency can be improved to  $\nu = 2^{n-1}/(2^n - 1)$  if more measurement settings (like the

$2^n - 1$  linearly independent stabilizers) are used. Since the stabilizer generators are Pauli operators, by Theorem 1, the sequential NDQV protocol  $\mathcal{M}$  can be realized using QND measurements with only two-body couplings  $\mathcal{C}_X$  and suitable local operations. These QND measurements can be implemented in the same way as the syndrome measurements for stabilizer quantum error correction codes [36].

Take the three-qubit GHZ state  $|\text{GHZ}_3\rangle = (|000\rangle + |111\rangle)/\sqrt{2}$ , where one set of the stabilizer generators are given by  $\{XXX, ZIZ, ZZI\}$ , as an example. We can construct the sequential NDQV protocol as  $\mathcal{M} = \mathcal{M}_1 \mathcal{M}_2 \mathcal{M}_3$  (or arbitrary permutations of the three measurement settings) with

$$\begin{aligned}\mathcal{M}_1 &= (\mathbb{1} \otimes |0\rangle\langle 0|) [(H \otimes H \otimes H \otimes \mathbb{1}) \\ &\quad \mathcal{C}_{X1a} \mathcal{C}_{X2a} \mathcal{C}_{X3a} (H \otimes H \otimes H \otimes \mathbb{1})], \\ \mathcal{M}_2 &= (\mathbb{1} \otimes |0\rangle\langle 0|) [\mathcal{C}_{X1a} \mathcal{C}_{X3a}], \\ \mathcal{M}_3 &= (\mathbb{1} \otimes |0\rangle\langle 0|) [\mathcal{C}_{X1a} \mathcal{C}_{X2a}].\end{aligned}\quad (20)$$

Again, simple direct calculations can prove that  $\mathcal{M}$  is equivalent to the optimal global strategy.

*Discussion.*—As compared to the standard QSV protocols, the sequential NDQV protocol  $\mathcal{M}$  offers two major advantages, namely, its optimal global efficiency and its robustness in the measurement setting sequence. These advantages come with the unavoidable cost of adding additional ancilla qubits as well as implementing coupling operations between the system and the ancilla. In a way, we replace the resources from preparing the state to be verified over and over again by the cheaper preparation of the ancilla state  $|0\rangle$  for each QND measurement. Experimentally, the realization of these QND measurements is considered to be a standard technique, and has been demonstrated in various platforms [38–44]. Moreover, Proposition 2 shows that only two-body couplings are needed in the sequential NDQV protocol, which can greatly simplify the experimental implementations. Nevertheless, one is still strongly encouraged to find the simplest implementations tailored to the specific problem and system at hand. For instance, the operation based on the property that the sideband Rabi rate depends only on the number of qubits in the ground state [45] can be useful to construct a simpler sequential NDQV protocol for verifying  $n$ -qubit Dicke states [18], otherwise it could be very complex if only two-body couplings are allowed.

One might find our sequential NDQV protocol similar to the adaptive QSV scheme which can also be regarded as being realized sequentially. However, they differ clearly in two major aspects. Firstly, the system is directly measured in the standard adaptive QSV scheme, whereas, in the sequential NDQV protocol, the measurements are done through the ancilla. Secondly, in the adaptive approach, the choice of the latter measurement depends on the previous measurement outcomes,

whereas the order of measurement settings in the sequential NDQV protocol can be arbitrary which eases its experimental implementations. Furthermore, the adaptive scheme can also be realized using QND measurements as demonstrated in Appendix D.

*Conclusion.*—We have presented a universally optimal protocol for quantum state verification using QND measurements. By virtue of the nondestructive feature of the QND measurements, we proposed the sequential NDQV protocol. Under such a design, not only can we preserve the target states, but also make our protocol equivalent to the optimal global strategy in terms of the verification efficiency. Moreover, our protocol is robust in the sense that the order of the sequential measurements can be arbitrarily constructed which is rather friendly to experimental implementations. We demonstrated the power of our protocol through three concrete examples. In addition, we proved that the protocol can also be used to perform tasks including fidelity estimation and state preparation. Lastly, by employing the state-process duality, our protocol can be extended to verifying quantum processes including quantum gates and quantum measurements [25].

We are grateful to Xiao-Dong Yu and Huangjun Zhu for helpful discussions. This work was supported by the National Key R&D Program of China under Grant No. 2017YFA0303800 and the National Natural Science Foundation of China through Grant Nos. 11574031, 61421001, and 11805010. J.S. also acknowledges support by the Beijing Institute of Technology Research Fund Program for Young Scholars. The Centre for Quantum Technologies is a Research Centre of Excellence funded by the Ministry of Education and the National Research Foundation of Singapore.

---

\* [jiangwei.shang@bit.edu.cn](mailto:jiangwei.shang@bit.edu.cn)  
 † [zhangxd@bit.edu.cn](mailto:zhangxd@bit.edu.cn)

[1] M. Paris and J. Řeháček, eds., *Quantum State Estimation*, Lecture Notes in Physics, Vol. 649 (Springer-Verlag Berlin Heidelberg, 2004).  
 [2] H. Häffner, W. Hänsel, C. F. Roos, J. Benhelm, D. Chekal-kar, M. Chwalla, T. Körber, U. D. Rapol, M. Riebe, P. O. Schmidt, C. Becher, O. Gühne, W. Dür, and R. Blatt, *Nature* **438**, 643 (2005).  
 [3] J. Shang, Z. Zhang, and H. K. Ng, *Phys. Rev. A* **95**, 062336 (2017).  
 [4] D. Mayers and A. Yao, *Quantum Inf. Comput.* **4**, 273 (2004).  
 [5] G. Tóth and O. Gühne, *Phys. Rev. Lett.* **94**, 060501 (2005).  
 [6] O. Gühne and G. Tóth, *Phys. Rep.* **474**, 1 (2009).  
 [7] S. T. Flammia and Y.-K. Liu, *Phys. Rev. Lett.* **106**, 230501 (2011).  
 [8] A. Dimić and B. Dakić, *npj Quantum Inf.* **4**, 11 (2018).  
 [9] S. Pallister, N. Linden, and A. Montanaro, *Phys. Rev. Lett.* **120**, 170502 (2018).  
 [10] M. Hayashi, K. Matsumoto, and Y. Tsuda, *J. Phys. A: Math. Gen.* **39**, 14427 (2006).  
 [11] T. Morimae, Y. Takeuchi, and M. Hayashi, *Phys. Rev. A* **96**, 062321 (2017).  
 [12] Y. Takeuchi and T. Morimae, *Phys. Rev. X* **8**, 021060 (2018).  
 [13] X.-D. Yu, J. Shang, and O. Gühne, *npj Quantum Inf.* **5**, 112 (2019).  
 [14] Z. Li, Y.-G. Han, and H. Zhu, *Phys. Rev. A* **100**, 032316 (2019).  
 [15] K. Wang and M. Hayashi, *Phys. Rev. A* **100**, 032315 (2019).  
 [16] H. Zhu and M. Hayashi, *Phys. Rev. A* **99**, 052346 (2019).  
 [17] H. Zhu and M. Hayashi, *Phys. Rev. Applied* **12**, 054047 (2019).  
 [18] Y.-C. Liu, X.-D. Yu, J. Shang, H. Zhu, and X. Zhang, *Phys. Rev. Applied* **12**, 044020 (2019).  
 [19] W.-H. Zhang, Z. Chen, X.-X. Peng, X.-Y. Xu, P. Yin, X.-J. Ye, J.-S. Xu, G. Chen, C.-F. Li, and G.-C. Guo, [arXiv:1905.12175](https://arxiv.org/abs/1905.12175).  
 [20] Z. Li, Y.-G. Han, and H. Zhu, [arXiv:1909.08979](https://arxiv.org/abs/1909.08979).  
 [21] H. Zhu and M. Hayashi, *Phys. Rev. Lett.* **123**, 260504 (2019).  
 [22] H. Zhu and M. Hayashi, *Phys. Rev. A* **100**, 062335 (2019).  
 [23] X. Jiang, K. Wang, K. Qian, Z. Chen, Z. Chen, L. Lu, L. Xia, F. Song, S. Zhu, and X. Ma, [arXiv:2002.00640](https://arxiv.org/abs/2002.00640).  
 [24] Z. Li, Y.-G. Han, H.-F. Sun, J. Shang, and H. Zhu, [arXiv:2004.06873](https://arxiv.org/abs/2004.06873).  
 [25] Y.-C. Liu, J. Shang, X.-D. Yu, and X. Zhang, *Phys. Rev. A* **101**, 042315 (2020).  
 [26] H. Zhu and H. Zhang, *Phys. Rev. A* **101**, 042316 (2020).  
 [27] P. Zeng, Y. Zhou, and Z. Liu, [arXiv:1911.06855](https://arxiv.org/abs/1911.06855).  
 [28] K. S. Thorne, R. W. P. Drever, C. M. Caves, M. Zimmerman, and V. D. Sandberg, *Phys. Rev. Lett.* **40**, 667 (1978).  
 [29] V. B. Braginsky, Y. I. Vorontsov, and K. S. Thorne, *Science* **209**, 547 (1980).  
 [30] T. C. Ralph, S. D. Bartlett, J. L. O'Brien, G. J. Pryde, and H. M. Wiseman, *Phys. Rev. A* **73**, 012113 (2006).  
 [31] G.-P. Guo, C.-F. Li, and G.-C. Guo, *Phys. Lett. A* **286**, 401 (2001).  
 [32] D. Gottesman, [arXiv:quant-ph/9705052](https://arxiv.org/abs/quant-ph/9705052).  
 [33] J. Preskill, in *Introduction to Quantum Computation and Information*, edited by H.-K. Lo, S. Popescu, and T. Spiller (World Scientific, Singapore, 1998) pp. 213–269.  
 [34] J. Chiaverini, D. Leibfried, T. Schaetz, M. D. Barrett, R. B. Blakestad, J. Britton, W. M. Itano, J. D. Jost, E. Knill, C. Langer, R. Ozeri, and D. J. Wineland, *Nature* **432**, 602 (2004).  
 [35] E. Knill, *Nature* **434**, 39 (2005).  
 [36] D. A. Lidar and T. A. Brun, eds., *Quantum Error Correction* (Cambridge University Press, 2013).  
 [37] D. Gottesman, *Phys. Rev. A* **54**, 1862 (1996).  
 [38] P. Grangier, J. A. Levenson, and J.-P. Poizat, *Nature* **396**, 537 (1998).  
 [39] G. Nogues, A. Rauschenbeutel, S. Osnaghi, M. Brune, J. Raimond, and S. Haroche, *Nature* **400**, 239 (1999).  
 [40] A. Lupascu, S. Saito, T. Picot, P. De Groot, C. Harmans, and J. Mooij, *Nat. Phys.* **3**, 119 (2007).  
 [41] J. Geremia, J. K. Stockton, and H. Mabuchi, *Science* **304**, 270 (2004).  
 [42] P. Neumann, J. Beck, M. Steiner, F. Rempp, H. Fedder,

P. R. Hemmer, J. Wrachtrup, and F. Jelezko, [Science](#) **329**, 542 (2010).

[43] L. Robledo, L. Childress, H. Bernien, B. Hensen, P. F. Alkemade, and R. Hanson, [Nature](#) **477**, 574 (2011).

[44] T. Nakajima, A. Noiri, J. Yoneda, M. R. Delbecq, P. Stano, T. Otsuka, K. Takeda, S. Amaha, G. Allison, K. Kawasaki, *et al.*, [Nat. Nanotechnol.](#) **14**, 555 (2019).

[45] D. B. Hume, T. Rosenband, and D. J. Wineland, [Phys. Rev. Lett.](#) **99**, 120502 (2007).

### Appendix A: The definition of $\nu(\mathcal{M})$

Without loss of generality, we consider the case that the actual state is  $\sigma = |\psi_\epsilon\rangle\langle\psi_\epsilon|$  with  $|\psi_\epsilon\rangle = \sqrt{1-\epsilon}|\psi\rangle + \sqrt{\epsilon}|\psi^\perp\rangle$ , where  $|\psi^\perp\rangle$  represents an arbitrary state orthogonal to  $|\psi\rangle$  and  $0 < \epsilon < 1$  is the infidelity. Then, the maximal probability for  $\sigma$  to pass the protocol  $\mathcal{M}$  is given by

$$\begin{aligned} & \max_{\langle\psi|\sigma|\psi\rangle \leq 1-\epsilon} \text{tr}[\mathcal{M}(\sigma \otimes |0\rangle\langle 0|)] \\ &= \max_{\mathcal{M}} \min_{|\psi^\perp\rangle} \text{tr} \left\{ (1-\epsilon)\mathcal{M}(|\psi\rangle\langle\psi| \otimes |0\rangle\langle 0|) + \epsilon\mathcal{M}(|\psi^\perp\rangle\langle\psi^\perp| \otimes |0\rangle\langle 0|) \right. \\ & \quad \left. + \sqrt{\epsilon}\sqrt{1-\epsilon}\mathcal{M}[(|\psi^\perp\rangle\langle\psi| + |\psi\rangle\langle\psi^\perp|) \otimes |0\rangle\langle 0|] \right\} \\ &= 1 - [1 - \lambda_2(\mathcal{M})]\epsilon, \end{aligned} \quad (21)$$

where  $\lambda_2(\mathcal{M})$  is the second largest eigenvalue of  $\mathcal{M}$  with the corresponding eigenstate  $|\psi^\perp\rangle \otimes |0\rangle$ . Hence, in order to verify the target state  $|\psi\rangle$  within infidelity  $\epsilon$  and confidence level  $1 - \delta$ , we need

$$N \approx \frac{1}{\nu(\mathcal{M})} \epsilon^{-1} \ln \delta^{-1} \quad (22)$$

copies of the states, where

$$\nu(\mathcal{M}) := 1 - \lambda_2(\mathcal{M}) \quad (23)$$

denotes the spectral gap between the largest and the second largest eigenvalues of  $\mathcal{M}$ .

### Appendix B: Proof of Corollary 1

*Proof.* Consider a new measurement setting with the general form  $\Omega_j = \lambda_0|\psi\rangle\langle\psi| + \sum_p \lambda_j^p|\psi^p\rangle\langle\psi^p|$ , where  $0 < \lambda_0 \leq 1$  as we allow  $\Omega_j$  to be a general positive operator-valued measure. Using Theorem 1, we construct the new sequential protocol as

$$\mathcal{M}' = \mathcal{M}\mathcal{M}_j \hat{=} \lambda_0|\psi\rangle\langle\psi| \otimes \mathbb{1}. \quad (24)$$

Hence, the new spectral gap is given by  $\nu(\mathcal{M}') = \lambda_0 \leq 1$ , meaning that the verification efficiency is not improved.  $\square$

### Appendix C: Standard QSV protocols for verifying arbitrary two-qubit pure states

#### 1. The non-adaptive approach

To verify an arbitrary two-qubit pure state  $|\Psi\rangle = \sin\theta|00\rangle + \cos\theta|11\rangle$  with  $\theta \in (0, \pi/4)$ , the standard QSV protocol with the optimal verification efficiency using only local and non-adaptive measurements contains four measurement settings [9], i.e.,

$$\Omega^{(4)} = \alpha(\theta)P_{ZZ}^+ + \frac{1-\alpha(\theta)}{3} \sum_{k=1}^3 [\mathbb{1} - |\phi_k\rangle\langle\phi_k|], \quad \text{for } \alpha(\theta) = \frac{2 - \sin(2\theta)}{4 + \sin(2\theta)}, \quad (25)$$

with the efficiency giving by  $\nu(\Omega^{(4)}) = 1/(2 + \sin\theta \cos\theta)$ . The first setting  $P_{ZZ}^+ = |00\rangle\langle 00| + |11\rangle\langle 11|$  is the projector onto the positive eigenspace of the Pauli measurement  $ZZ$ , and the rest three  $\mathbb{1} - |\phi_k\rangle\langle\phi_k|$  are the measurements that

reject the state  $|\phi_k\rangle$  where

$$|\phi_1\rangle = \left( \frac{1}{\sqrt{1+\tan\theta}}|0\rangle + \frac{e^{\frac{2\pi i}{3}}}{\sqrt{1+\cot\theta}}|1\rangle \right) \otimes \left( \frac{1}{\sqrt{1+\tan\theta}}|0\rangle + \frac{e^{\frac{\pi i}{3}}}{\sqrt{1+\cot\theta}}|1\rangle \right), \quad (26)$$

$$|\phi_2\rangle = \left( \frac{1}{\sqrt{1+\tan\theta}}|0\rangle + \frac{e^{\frac{4\pi i}{3}}}{\sqrt{1+\cot\theta}}|1\rangle \right) \otimes \left( \frac{1}{\sqrt{1+\tan\theta}}|0\rangle + \frac{e^{\frac{5\pi i}{3}}}{\sqrt{1+\cot\theta}}|1\rangle \right), \quad (27)$$

$$|\phi_3\rangle = \left( \frac{1}{\sqrt{1+\tan\theta}}|0\rangle + \frac{1}{\sqrt{1+\cot\theta}}|1\rangle \right) \otimes \left( \frac{1}{\sqrt{1+\tan\theta}}|0\rangle - \frac{1}{\sqrt{1+\cot\theta}}|1\rangle \right). \quad (28)$$

However, as we show in Eq. (16) of the main text, to verify  $|\Psi\rangle$  using only local and non-adaptive measurements, a minimal three measurement settings are enough, which are

$$\begin{aligned} \Omega_1 &= P_{ZZ}^+ = |0\rangle\langle 0| \otimes |0\rangle\langle 0| + |1\rangle\langle 1| \otimes |1\rangle\langle 1|, \\ \Omega_2 &= \mathbb{1} - |+\rangle\langle +| \otimes |\varphi_+\rangle\langle\varphi_+|, \\ \Omega_3 &= \mathbb{1} - |-\rangle\langle -| \otimes |\varphi_-\rangle\langle\varphi_-|, \end{aligned} \quad (29)$$

where  $|\pm\rangle = (|0\rangle \pm |1\rangle)/\sqrt{2}$  and  $|\varphi_\pm\rangle = \cos\theta|0\rangle \mp \sin\theta|1\rangle$ . The latter two  $\Omega_{2(3)}$  are the measurements that reject the input states if getting  $|+\rangle$  ( $|-\rangle$ ) on the first subsystem and  $|\varphi_+\rangle$  ( $|\varphi_-\rangle$ ) on the second one simultaneously. Thus, such a protocol can be constructed as

$$\Omega^{(3)} = \Omega_{2qb} = \frac{1}{3}(\Omega_1 + \Omega_2 + \Omega_3), \quad (30)$$

with the efficiency  $\nu(\Omega^{(3)}) = 1/3$  which is independent of the parameter  $\theta$  and only a little worse than that of  $\Omega^{(4)}$ .

## 2. The adaptive approach

Furthermore, using the general transformation between the adaptive and non-adaptive schemes as presented in Ref. [18], the least number of measurement settings for verifying  $|\Psi\rangle$  can be reduced to only two by replacing  $\Omega_2$  and  $\Omega_3$  in  $\Omega^{(3)}$  with a single adaptive measurement

$$X_\Psi = |+\rangle\langle +| \otimes |\varphi_+^\perp\rangle\langle\varphi_+^\perp| + |-\rangle\langle -| \otimes |\varphi_-^\perp\rangle\langle\varphi_-^\perp|, \quad (31)$$

where  $|\varphi_\pm^\perp\rangle = \sin\theta|0\rangle \pm \cos\theta|1\rangle$ . Then we have the protocol

$$\Omega_{\text{adp}}^{(2)} = \frac{1}{2}P_{ZZ}^+ + \frac{1}{2}X_\Psi, \quad (32)$$

which improves the verification efficiency to  $\nu(\Omega_{\text{adp}}^{(2)}) = 1/2$ .

Last but not least, we note that using adaptive measurements, an optimal efficiency can be achieved by considering the symmetry between the measurement settings. Such a protocol with three measurement settings has been proposed and proven in Ref. [13],

$$\Omega_{\text{adp}}^{(3)} = \frac{\cos^2\theta}{1+\cos^2\theta}P_{ZZ}^+ + \frac{1}{2(1+\cos^2\theta)}X_\Psi + \frac{1}{2(1+\cos^2\theta)}Y_\Psi, \quad (33)$$

where

$$\begin{aligned} P_{ZZ}^+ &= |0\rangle\langle 0| \otimes |0\rangle\langle 0| + |1\rangle\langle 1| \otimes |1\rangle\langle 1|, \\ X_\Psi &= |\varphi_0\rangle\langle\varphi_0| + |\varphi_2\rangle\langle\varphi_2|, \\ Y_\Psi &= |\varphi_1\rangle\langle\varphi_1| + |\varphi_3\rangle\langle\varphi_3|, \end{aligned} \quad (34)$$

with  $|\varphi_0\rangle = \frac{1}{\sqrt{2}}(|0\rangle + |1\rangle) \otimes (\sin\theta|0\rangle + \cos\theta|1\rangle)$  and  $|\varphi_k\rangle = g^k|\varphi_0\rangle$ . The unitary operator  $g$  is defined as  $g = \Upsilon \otimes \Upsilon^\dagger$ , where  $\Upsilon$  is the phase gate, i.e.,  $\Upsilon|0\rangle = |0\rangle$  and  $\Upsilon|1\rangle = i|1\rangle$ . Note that  $X_\Psi$  is the same as that in Eq. (31). Then the optimal efficiency with adaptive measurements is given by  $\nu(\Omega_{\text{adp}}^{(3)}) = 1/(1+\cos^2\theta)$ .

## Appendix D: Adaptive QND measurements

We use the measurement setting

$$X_\Psi = |+\rangle\langle+| \otimes |\varphi_+^\perp\rangle\langle\varphi_+^\perp| + |-\rangle\langle-| \otimes |\varphi_-^\perp\rangle\langle\varphi_-^\perp| \quad (35)$$

in Eq. (31) as an example to demonstrate how to realize adaptive measurements using the non-demolition approach. Since the measurements in standard QSV protocols are expected to be local, one can first rotate them to the measurement basis  $\{|0\rangle, |1\rangle\}$ , which can then be realized by the QND measurements  $\{(\mathbb{1} \otimes |0\rangle\langle 0|)\mathcal{C}_X, (\mathbb{1} \otimes |1\rangle\langle 1|)\mathcal{C}_X\}$  straightforwardly. Such rotations for the two adaptive measurements in  $X_\Psi$  are given by

$$\begin{aligned} (H \otimes R_+)(|+\rangle\langle+| \otimes |\varphi_+^\perp\rangle\langle\varphi_+^\perp|)(H \otimes R_+)^{\dagger} &= |0\rangle\langle 0| \otimes |0\rangle\langle 0|, \\ (H \otimes R_-)(|-\rangle\langle-| \otimes |\varphi_-^\perp\rangle\langle\varphi_-^\perp|)(H \otimes R_-)^{\dagger} &= |1\rangle\langle 1| \otimes |0\rangle\langle 0|, \end{aligned} \quad (36)$$

where  $H$  is the Hadamard gate and  $R_\pm$  are rotations that turn the state  $|\varphi_\pm^\perp\rangle$  into  $|0\rangle$ . Specifically, we have

$$R_+ = \begin{bmatrix} \sin \theta & \cos \theta \\ -\cos \theta & \sin \theta \end{bmatrix}, \quad R_- = \begin{bmatrix} \sin \theta & -\cos \theta \\ \cos \theta & \sin \theta \end{bmatrix}. \quad (37)$$

Then, the adaptive QND measurements for  $X_\Psi$  can be constructed as

$$\begin{aligned} \mathcal{M}_{X_\Psi} &= (H \otimes R_+^\dagger \otimes \mathbb{1})(\mathbb{1} \otimes |0\rangle\langle 0|)\mathcal{C}_{X2a'}(\mathbb{1} \otimes R_+ \otimes \mathbb{1})(\mathbb{1} \otimes |0\rangle\langle 0|)\mathcal{C}_{X1a}(H \otimes \mathbb{1} \otimes \mathbb{1}) \\ &\quad + (H \otimes R_-^\dagger \otimes \mathbb{1})(\mathbb{1} \otimes |0\rangle\langle 0|)\mathcal{C}_{X2a'}(\mathbb{1} \otimes R_- \otimes X)(\mathbb{1} \otimes |1\rangle\langle 1|)\mathcal{C}_{X1a}(H \otimes \mathbb{1} \otimes \mathbb{1}). \end{aligned} \quad (38)$$

Note that  $\mathcal{M}_{X_\Psi}$  contains two terms, because  $X_\Psi$  is an adaptive measurement with two branches.

Specifically, the whole measurement process consists of two steps. The first step is to realize the QND version of the two-outcome projective measurement  $\{|+\rangle\langle+|, |-\rangle\langle-|\}$  on the first particle. The second is to realize the QND version of the adaptive projective measurement  $|\varphi_+^\perp\rangle\langle\varphi_+^\perp|$  or  $|\varphi_-^\perp\rangle\langle\varphi_-^\perp|$  on the second particle according to the outcome of the first step. To be specific, we rotate the first particle with a Hadamard gate  $H$  and send it to a CNOT gate  $\mathcal{C}_X$  together with an ancilla qubit  $a$  in state  $|0\rangle$ . Then we measure the ancilla qubit using a Pauli- $Z$  measurement. If the outcome is  $|0\rangle$  (or  $|1\rangle$ ), we rotate the second particle by  $R_+$  (or  $R_-$ ) and send it to another CNOT gate together with a new ancilla qubit  $a'$  in state  $|0\rangle$ . After that, the ancilla is measured by a Pauli- $Z$  measurement, and we declare the test passes if the outcome  $|0\rangle$  is obtained. Finally, the state is rotated back to its original form. Note that the last rotation commutes with the second measurement, so that we can conveniently choose to do the measurement in the very end. This results in the alternative writing of Eq. (38), i.e.,

$$\begin{aligned} \mathcal{M}_{X_\Psi} &= (\mathbb{1} \otimes |00\rangle\langle 00|)(H \otimes R_+^\dagger \otimes \mathbb{1})\mathcal{C}_{X2a'}(\mathbb{1} \otimes R_+ \otimes \mathbb{1})\mathcal{C}_{X1a}(H \otimes \mathbb{1} \otimes \mathbb{1}) \\ &\quad + (\mathbb{1} \otimes |01\rangle\langle 01|)(H \otimes R_-^\dagger \otimes \mathbb{1})\mathcal{C}_{X2a'}(\mathbb{1} \otimes R_- \otimes X)\mathcal{C}_{X1a}(H \otimes \mathbb{1} \otimes \mathbb{1}). \end{aligned} \quad (39)$$

## Appendix E: Proof of Proposition 2

*Proof.* Without loss of generality, we consider the generalized controlled- $X$  gate  $\mathcal{C}_X^n$  such that the ancilla qubit is controlled by  $n$  system qubits, i.e.,

$$\mathcal{C}_X^n = (\mathbb{1} - |11\cdots 1\rangle\langle 11\cdots 1|) \otimes \mathbb{1} + |11\cdots 1\rangle\langle 11\cdots 1| \otimes X. \quad (40)$$

Note that the CNOT gate  $\mathcal{C}_X$  represents a special case of  $\mathcal{C}_X^n$  when  $n = 1$ , namely

$$\mathcal{C}_X = |0\rangle\langle 0| \otimes \mathbb{1} + |1\rangle\langle 1| \otimes X. \quad (41)$$

Following Eq. (11), for an arbitrary input state  $\sigma$  together with an ancilla qubit  $|0\rangle$ , the QND measurement with CNOT gates has the relation

$$[(\mathbb{1} \otimes |0\rangle\langle 0|)\mathcal{C}_X](\sigma \otimes |0\rangle\langle 0|) = (|0\rangle\langle 0| \otimes |0\rangle\langle 0| + |1\rangle\langle 1| \otimes |0\rangle\langle 1|)(\sigma \otimes |0\rangle\langle 0|) = (|0\rangle\langle 0| \otimes \mathbb{1})(\sigma \otimes |0\rangle\langle 0|), \quad (42)$$

which tells us that  $(\mathbb{1} \otimes |0\rangle\langle 0|)\mathcal{C}_X \hat{=} |0\rangle\langle 0| \otimes \mathbb{1}$ . Then, the sequential measurement constructed using  $n$  CNOT gates gives

$$[(\mathbb{1} \otimes |0\rangle\langle 0|)\mathcal{C}_{X1a}][(\mathbb{1} \otimes |0\rangle\langle 0|)\mathcal{C}_{X2a}] \cdots [(\mathbb{1} \otimes |0\rangle\langle 0|)\mathcal{C}_{Xna}] \hat{=} |00\cdots 0\rangle\langle 00\cdots 0| \otimes \mathbb{1}. \quad (43)$$

With the rotation of a Pauli- $X$  measurement, the generalized controlled- $X$  gate becomes

$$(X \otimes X \otimes \cdots \otimes X \otimes \mathbb{1})\mathcal{C}_X^n(X \otimes X \otimes \cdots \otimes X \otimes \mathbb{1}) = (\mathbb{1} - |00\cdots0\rangle\langle 00\cdots0|) \otimes \mathbb{1} + |00\cdots0\rangle\langle 00\cdots0| \otimes X, \quad (44)$$

so that the QND measurement with rotated  $\mathcal{C}_X^n$  has the equivalence

$$(\mathbb{1} \otimes |0\rangle\langle 0|)(X \otimes X \otimes \cdots \otimes X \otimes \mathbb{1})\mathcal{C}_X^n(X \otimes X \otimes \cdots \otimes X \otimes \mathbb{1}) \hat{=} (\mathbb{1} - |00\cdots0\rangle\langle 00\cdots0|) \otimes \mathbb{1}. \quad (45)$$

Following Eqs. (43) and (45), one can quickly find

$$\begin{aligned} & (\mathbb{1} \otimes |0\rangle\langle 0|)(X \otimes X \otimes \cdots \otimes X \otimes \mathbb{1})\mathcal{C}_X^n(X \otimes X \otimes \cdots \otimes X \otimes \mathbb{1}) \\ & \hat{=} \mathbb{1} - [(\mathbb{1} \otimes |0\rangle\langle 0|)\mathcal{C}_{X1a}] [(\mathbb{1} \otimes |0\rangle\langle 0|)\mathcal{C}_{X2a}] \cdots [(\mathbb{1} \otimes |0\rangle\langle 0|)\mathcal{C}_{Xna}], \end{aligned} \quad (46)$$

which means that  $(n+1)$ -body couplings can always be realized by  $n$  times the sequential measurements constituted by two-body couplings only with non-demolition measurements.

Now we can generalize the proof by considering the  $(n+1)$ -body coupling in the form of

$$R\mathcal{C}_X^n := (R^{(1)\dagger} \otimes R^{(2)\dagger} \otimes \cdots \otimes R^{(n)\dagger} \otimes \mathbb{1})\mathcal{C}_X^n(R^{(1)} \otimes R^{(2)} \otimes \cdots \otimes R^{(n)} \otimes \mathbb{1}) = (nR \otimes \mathbb{1})\mathcal{C}_X^n(nR^\dagger \otimes \mathbb{1}), \quad (47)$$

where  $R^{(i)}$ s are arbitrary local unitary operations. One notes that as the initial state of the target qubit, which is the ancilla, in the QND measurements is fixed to be  $|0\rangle$ , the local operator  $R^{(a)} = \mathbb{1}$ . Similarly, for a two-body coupling controlled by system qubit  $i$  and targeted on ancilla qubit  $a$ , we have

$$R\mathcal{C}_{Xia} := (R^{(i)\dagger} \otimes \mathbb{1})\mathcal{C}_{Xia}(R^{(i)} \otimes \mathbb{1}) \hat{=} |\phi_i\rangle\langle\phi_i| \otimes \mathbb{1}, \quad (48)$$

where  $|\phi_i\rangle = R^{(i)\dagger}|0\rangle$ . So we have the QND measurements

$$nR\mathcal{M}_X := [(\mathbb{1} \otimes |0\rangle\langle 0|)R\mathcal{C}_{X1a}] [(\mathbb{1} \otimes |0\rangle\langle 0|)R\mathcal{C}_{X2a}] \cdots [(\mathbb{1} \otimes |0\rangle\langle 0|)R\mathcal{C}_{Xna}] \hat{=} |\phi\rangle\langle\phi| \otimes \mathbb{1}, \quad (49)$$

with  $|\phi\rangle = \bigotimes_i |\phi_i\rangle$ . Also, we can define the QND measurements

$$R\mathcal{M}_X^n := (X \otimes X \otimes \cdots \otimes X \otimes \mathbb{1})R\mathcal{C}_X^n(X \otimes X \otimes \cdots \otimes X \otimes \mathbb{1}) \hat{=} (\mathbb{1} - |\phi\rangle\langle\phi|) \otimes \mathbb{1}. \quad (50)$$

Then one can quickly obtain the more general relation

$$R\mathcal{M}_X^n \hat{=} \mathbb{1} - nR\mathcal{M}_X. \quad (51)$$

Note that the effective commutation between the projective measurement  $\mathbb{1} \otimes |0\rangle\langle 0|$  and the local operations  $R^i$  and Pauli- $X$ , as well as the commutation between  $\mathcal{C}_{Xia}$  and  $R^{(j)}$  ( $i \neq j$ ) can help us move the operators around and simplify the experimental realizations.

For example, the QND measurement using CNOT gates for verifying arbitrary two-qubit pure states with the order of Eq. (19) in the main text is

$$\mathcal{M}_i^b = \mathbb{1} - (\mathbb{1} \otimes |00\rangle\langle 00|)(R_i^\dagger \otimes \mathbb{1})\mathcal{C}_{X1a}\mathcal{C}_{X2a'}(R_i \otimes \mathbb{1}), \quad (52)$$

which can easily be realized with four steps using two ancilla qubits initialized as  $|00\rangle$ : two local rotations, two couplings, two local rotations, and two ancilla measurements. However, it can also be rewritten as

$$\mathcal{M}_i^{b'} = \mathbb{1} - [(\mathbb{1} \otimes |0\rangle\langle 0|)(R_i^{(1)\dagger} \otimes \mathbb{1})\mathcal{C}_{X1a}(R_i^{(1)} \otimes \mathbb{1})] [(\mathbb{1} \otimes |0\rangle\langle 0|)(R_i^{(2)\dagger} \otimes \mathbb{1})\mathcal{C}_{X2a'}(R_i^{(2)} \otimes \mathbb{1})], \quad (53)$$

where  $R_i = R_i^{(1)} \otimes R_i^{(2)}$ . This order is in favor of modular designs that can be constructed by the same blocks on the two qubits with four steps: one local rotation, one coupling between the two qubits, one local rotation, and one ancilla measurement. Such blocks can be conveniently extended for the verification of other multipartite entangled states. Moreover, only one ancilla qubit is required if it can be re-initialized during the experiment.  $\square$